ARDARA™
www.ArdaraTech.com

# Practical Quadrupole Theory: Surface Induced Dissociation (SID) Energetics Characterization

Luke J. Metzler and Randall E. Pedder, Ardara Technologies L.P., Ardara, PA, USA

## Introduction

Surface Induced Dissociation (SID) is well recognized to provide analytical information about chemical species, via MS/MS.

Compared with Collision Induced Dissociation (CID), SID promises more reproducible energy resolved breakdown curves, and access to higher energy fragmentation pathways, which can increase selectivity for MS/MS experiments. However, CID generally has much better conversion efficiency of parent to progeny ions (approaching 100% in some cases involving ion traps), which in turn increases ultimate sensitivity.

MS/MS using a tandem quadrupole configuration promises less ambiguous results than in an ion trap configuration due to the ion trap's potential complications of space charge and ion molecule reactions.

This work explores the analytical utility of SID for tandem quadrupole MS/MS, both in selectivity and sensitivity.

## Experimental

A component electrospray quadrupole mass spectrometer was configured with a 9.25mm resolving quadrupole, followed by an in-line SID collision cell, followed by a collision-free RF-only rectilinear quadrupole ion guide, leading into a second 9.25 mm resolving quadrupole mass filter and electron multiplier detector. See Figure 1.

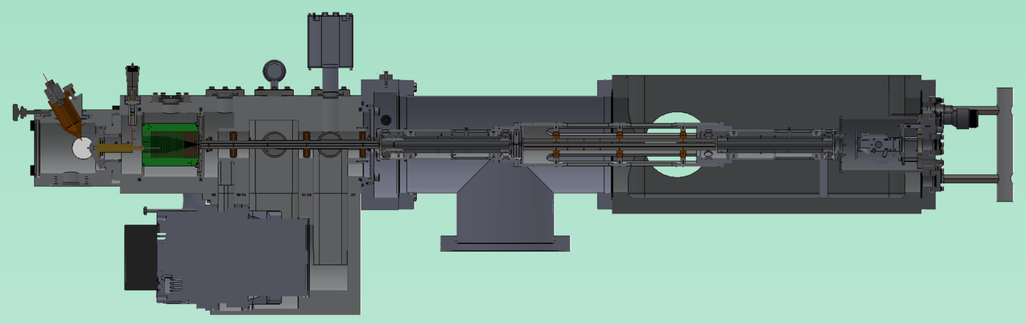

**Figure 1.** Electrospray Q-SID-Q mass spectrometer system.

The collision energy of the parent ions was varied by changing the voltages applied to the SID optics (See Figure 2), and the resulting ion energy profiles of the progeny ions was evaluated for various species by varying the pole bias offset of the downstream quadrupole mass filter in the form of a stopping potential experiment.

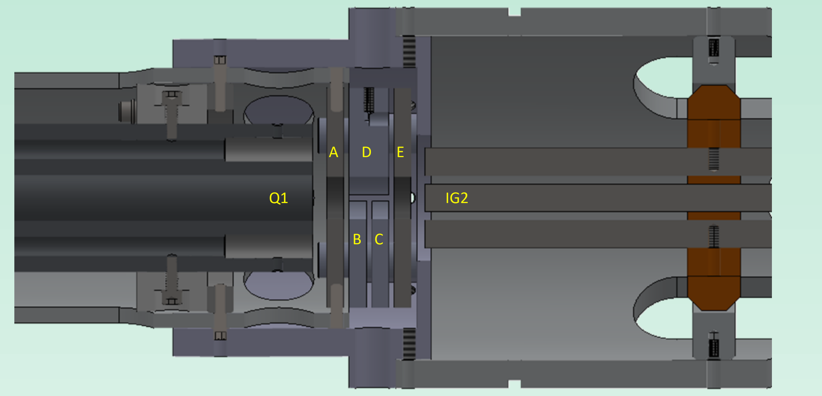


**Figure 2.** Detail showing the SID cell, including the first resolving quadrupole (Q1), the SID entrance lens (A), Deflectors 1 and 2 (B, C respectively), the SID surface (D), the SID exit lens (E), and the collision free ion guide (IG2).

In addition, by slowing down the ions as they traverse the ion guide and downstream quadrupole mass filter, information can be gleaned about the fragmentation dynamics.

The vacuum chamber was designed to mate to an Edwards Vacuum turbomolecular cartridge pump with booster stage, which was mounted into a custom designed housing with three planar rectangular vacuum ports. These vacuum ports align underneath the three rectangular vacuum ports of the ion guide chamber. The pumping speed on these three ports was 20 L/s, 200 L/s, and 200 L/s respectively, with the booster stage upgrading a 12 CFM mechanical pump to have 26 CFM pumping speed. The chamber configuration utilizes the insulating collars as conductance limits between the three distinct pumped regions (~30 millitorr, ~2 millitorr, and ~0.2 millitorr respectively).

The electrospray sprayer allows x, y, and z movement to optimize ion transmission to a four inch long heated stainless steel capillary with 0.020 inch inner diameter. The outlet of the stainless steel capillary exits into an ion funnel whose inner diameter ranges from 1.00 inches at its entrance to 0.070 inches at the ion funnel exit, with a 0.080 (2mm) conductance-limiting exit aperture. The ion funnel was operated at 2.4 MHz for all experiments, powered by an Ardara Technologies model 124 self-oscillating RF power supply, and was operated at a pressure of 1.6 to 1.7 torr for all experiments.

**Table 1. Typical ion transmission through the Ardara Technologies ESI Front-end**

| Element where ion current was measured | Ion current |
|---|---|
| ESI Needle (@ Front panel meter on ESI PS) | 110 nA |
| Ion Funnel (Preamplifier @ 10^9 gain) | 0.77* nA |
| Ion Guide (Preamplifier @ 10^9 gain) | 0.79 nA |
| Faraday Plate downstream of Ion Guide (Preamplifier @ 10^9 gain) | 0.76 nA |
| *Some ions may pass through the ion funnel exit aperture instead of contacting the electrodes, and therefore are not accounted for in this measurement | |

Solutions of phenethylamine (5μM), leucine enkephalin (5μM), and reserpine (5μM), in a 49.5 : 49.5 : 1 mixture of methanol, water, and formic acid were prepared for use in all of the following experiments.

The collision surface used in the SID cell consisted of a machined copper surface, which was polished to a mirror finish, de-oxidized by submersion in an argon-sparged dilute nitric acid solution, and coated with a monolayer of 2-perfluorohexyl ethyl thiol by submersion in a 1 mM solution of the thiol in isopropyl alcohol. The monolayer was assumed to be present when the copper surface completely repelled water after sonication in warm isopropanol for 20 minutes.

A SIMION model of the SID ion optics (see Figures 3 & 4), along with the upstream resolving quadrupole (Q1) and the collision-free ion guide (IG2), was created along with a LUA script to simulate the RF fields of Q1 and IG2. The secondary emission example library provided with the SIMION software was used to simulate the production of SID product ions. The tune used in the SIMION model is shown below in Table 2.

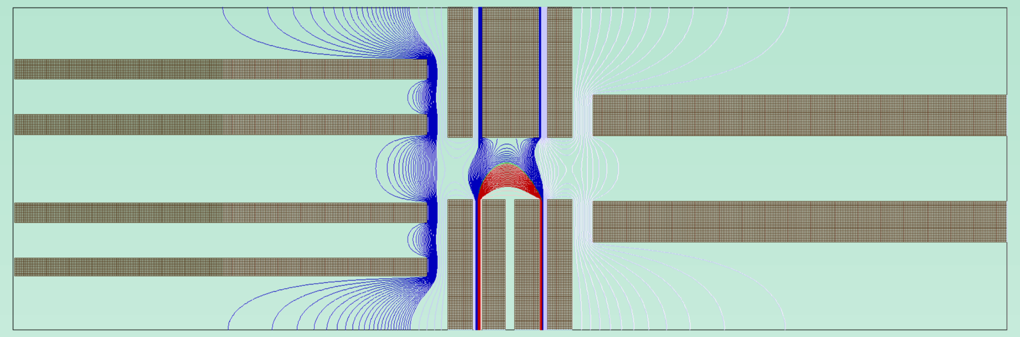

**Figure 3. SIMION simulation of the SID cell showing the equipotential contours for one of the tunes actually used in the experiments. Green is 0V, dark red is 1 to 25 V in 1 V increments, light red is 25 to 40 V in 5 V increments, blue is -1 to -25 V in 1 V increments, and light blue is –25 to –90 V in 5 V increments.**

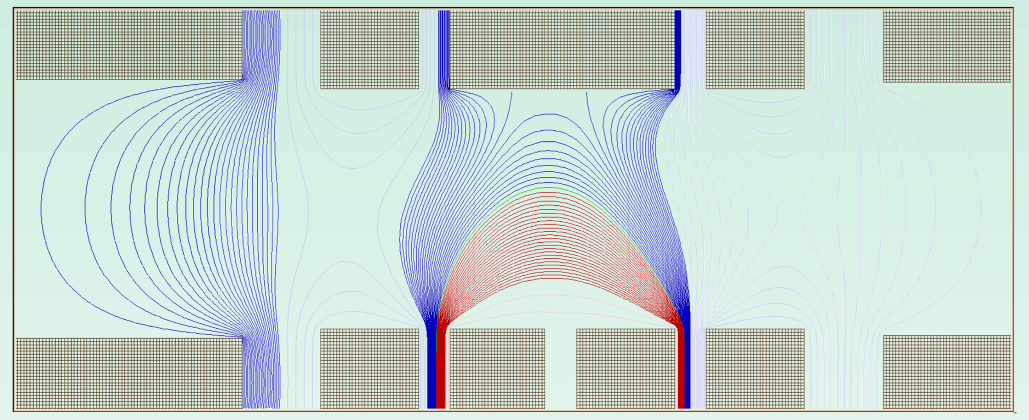

**Figure 4. Detail of SIMION simulation of the SID cell showing the equipotential contours for one of the tunes actually used in the experiments. Contours as above.**

**Table 2. The parameters of the tune simulated in SIMION and used to collect data.**

| | Pass-Through | SID Fragmentation |
|---|---|---|
| Q1 (9.25mm, 1.3 MHz) | 0V DC offset, ~1600 Vpp | 0V DC offset, ~1600 Vpp |
| SID Entrance Lens | -50 V | -50 V |
| SID Collision Surface | -10 V | -10 V |
| SID Deflector 1 | -10 V | 40 V |
| SID Deflector 2 | -10 V | 40 V |
| SID Exit Lens | -90 V | -90 V |
| IG2 (10mm rect., 3 MHz) | -30 V DC offset, 1200 Vpp | -30 V DC offset, 1200 Vpp |

## Results and Discussion:

MS/MS Conversion Efficiency can be defined as the total ion current of all progeny ions divided by the ion current of the parent ion, usually expressed as a percentage. The results of the SIMION simulation suggested that a tune existed that would provide approximately 20% conversion/transmission of fragment ions off the surface to the collision-free ion guide (See Figure 5). The simulation also demonstrated that, while intended to be used independently, the deflector lenses could be electrically connected and used as a single lens. Additionally, a reversal of the voltages of the SID surface and the deflector lens pair could potentially allow for fragmentation on the surface of the deflector lenses with similar conversion efficiency (See Figure 6.)

Initial experimental results demonstrated subtle differences between the fragmentation of protonated leucine enkephalin (YGGFL) at varying collision energy (See Figure 7.) Differences between the fragmentation on the copper surface and stainless steel surfaces were observed for protonated leucine enkephalin (Figure 8), protonated reserpine (Figure 9), and protonated phenethylamine (Figure 10), and conversion efficiencies of 15-20% agree well with the SIMION model.

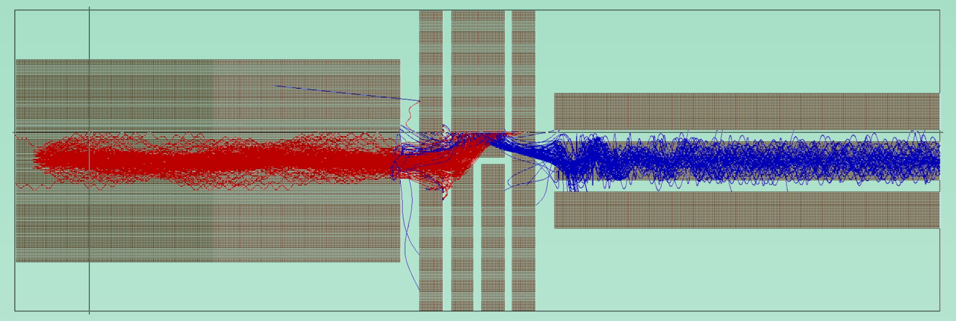

**Figure 5. SIMION simulation of the SID cell, showing ions (m/z 556) colliding with the copper (upper) surface (-10 volts potential), and fragmenting into secondary ions (m/z 221). The effective birth potential of the precursor ions was +20 volts, and the potential at the copper surface was -10 volts for an effective collision energy of 30 eV. This model suggests approximately 20% conversion/transmission efficiency for this fragment ion, assuming the product ion retains a small fraction of the energy of the precursor.**

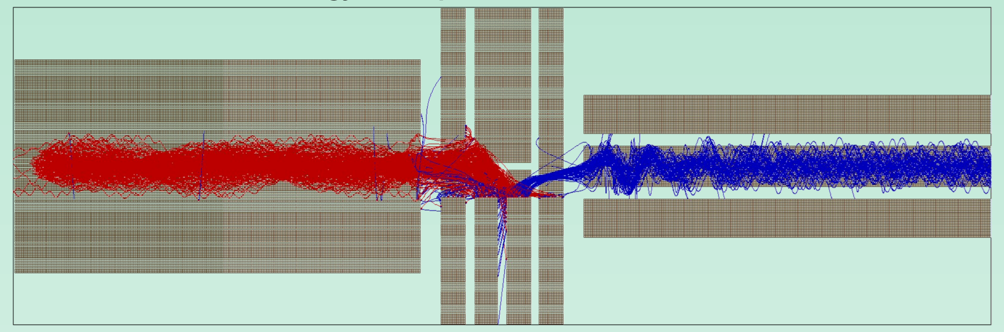

**Figure 6. Reversing the polarity of the SID electrodes SIMION simulation of the SID cell, showing ions (m/z 556) colliding with the stainless lens (lower) surfaces (-10 volts potential), and fragmenting into secondary ions (m/z 221). This model suggests approximately 16% conversion/transmission efficiency for this fragment ion, assuming the product ion retains a small fraction of the energy of the precursor. The reduction in conversion/transmission efficiency is presumably due to the presence of the gap between the two lower electrodes.**

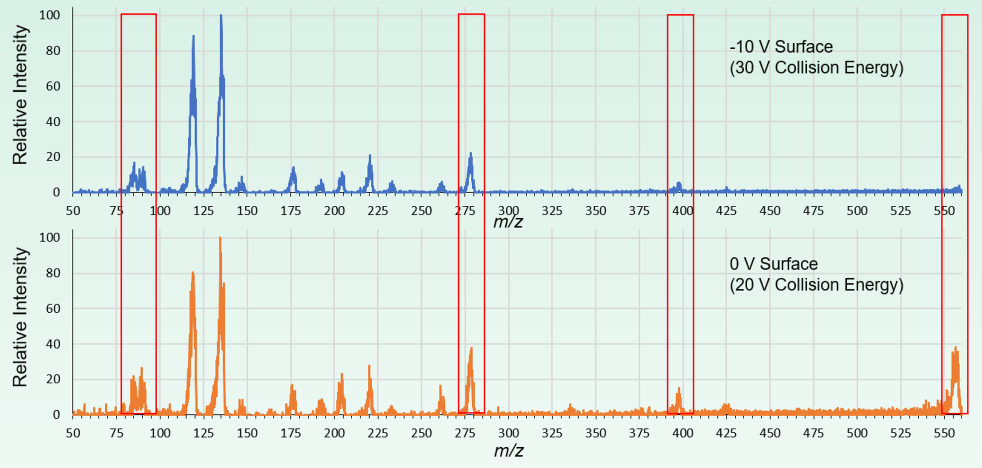


**Figure 7. Comparison the the SID fragmentation of m/z 556 [YGGFL+H]$^+$, isolated in Q1, impacting the copper SID surface at –10V and 0V. Differences in the relative intensities for various fragments can be observed, and the surviving m/z 556 in the 0V condition was stopped by a 2V pole bias on Q3, indicating that these ions impacted the surface, but did not gain sufficient energy to undergo fragmentation.**

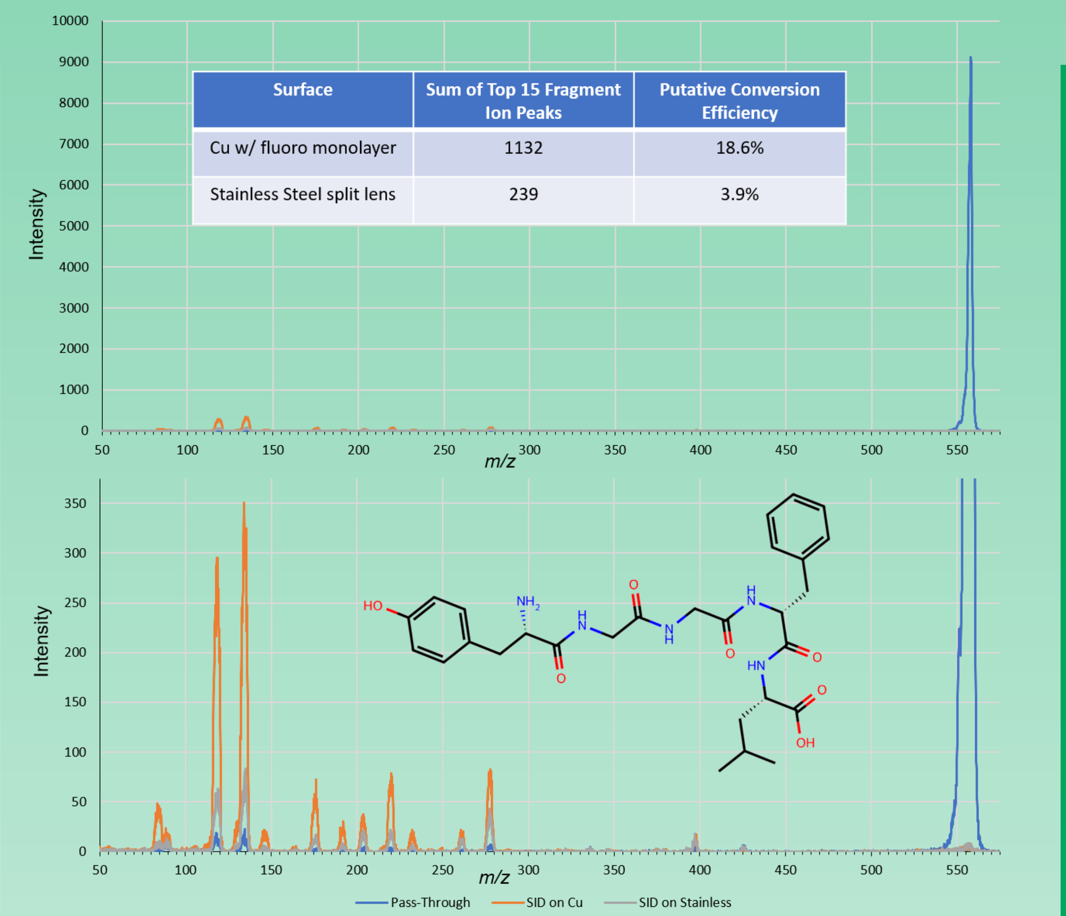


| Surface | Sum of Top 15 Fragment Ion Peaks | Putative Conversion Efficiency |
|---|---|---|
| Cu w/ fluoro monolayer | 1132 | 18.6% |
| Stainless Steel split lens | 239 | 3.9% |

**Figure 8. Mass spectra collected of isolated leucine enkephalin, m/z 556, [YGGFL+H]$^+$, showing the initial precursor ion intensity (blue) and the SID fragments observed after collision with the -10V copper surface (orange) and the -10V stainless steel surface (gray).**

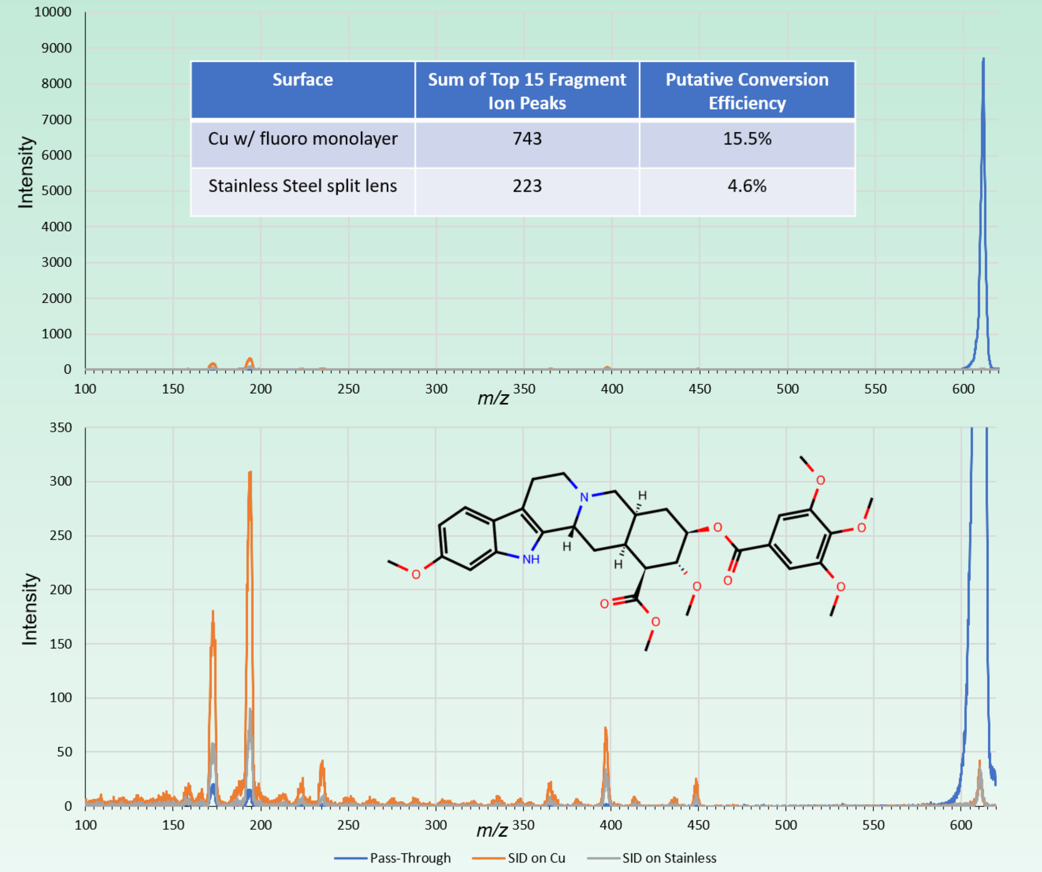


| Surface | Sum of Top 15 Fragment Ion Peaks | Putative Conversion Efficiency |
|---|---|---|
| Cu w/ fluoro monolayer | 743 | 15.5% |
| Stainless Steel split lens | 223 | 4.6% |

**Figure 9. Mass spectra collected of reserpine, m/z 609, [$C_{33}H_{40}N_2O_9$ +H]$^+$, showing the initial precursor ion intensity (blue) and the SID fragments observed after collision with the -10V copper surface (orange) and the -10V stainless steel surface (gray).**

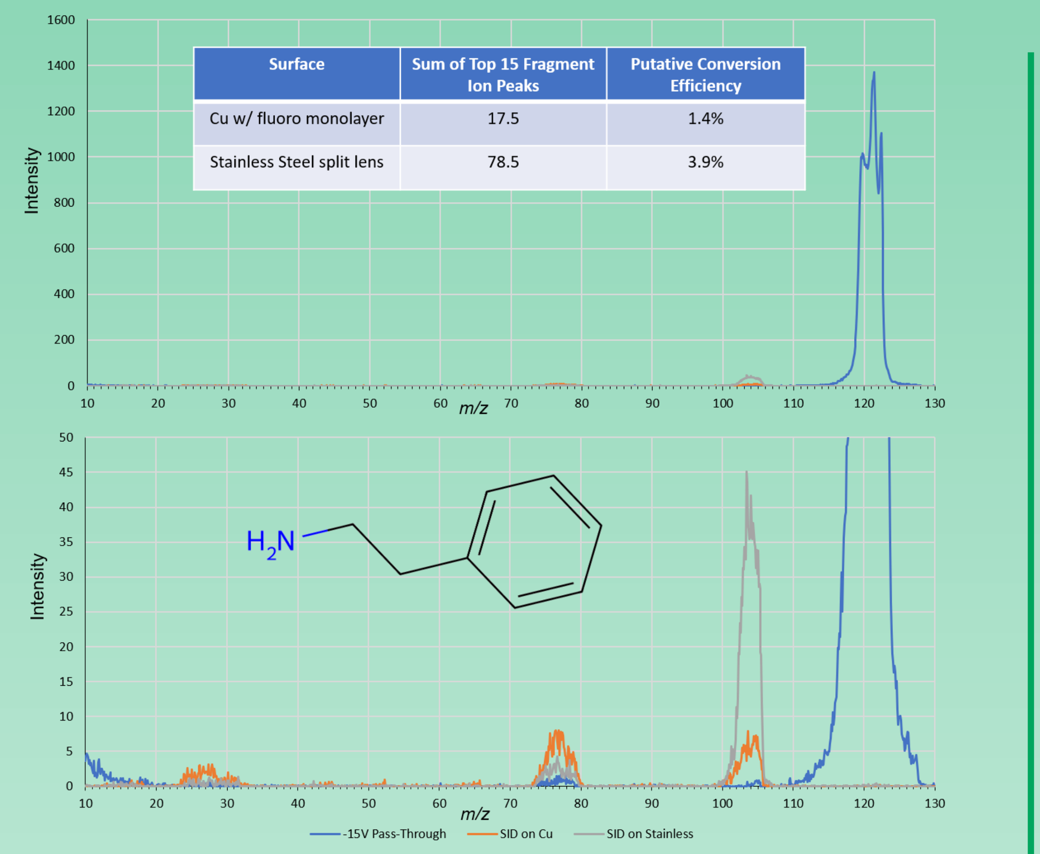


| Surface | Sum of Top 15 Fragment Ion Peaks | Putative Conversion Efficiency |
|---|---|---|
| Cu w/ fluoro monolayer | 17.5 | 1.4% |
| Stainless Steel split lens | 78.5 | 3.9% |

**Figure 10. Mass spectra collected of phenethylamine, m/z 122, [$C_8H_{11}N$+H]$^+$, showing the initial precursor ion intensity (blue) and the SID fragments observed after collision with the -10V copper surface (orange) and the -10V stainless steel surface (gray).**

The energy distribution of an ion beam can be experimentally measured by presenting and ion optically thick stopping potential somewhere along the ion optics path to the detector. In this configuration, the pole bias of the downstream quadrupole mass filter was varied in a step-wise fashion, and the ion current loss from each step measured and plotted as a 'first derivative curve', approximating the first derivative by a simple calculation of the experimentally measured 'instantaneous slope' (ΔY divided by ΔX) plotted as a function of stopping potential. The resulting first derivative curve represents a histogram showing the energy distribution of the ion beam, along with a measurement of its effective birth potential. The choice of using quadrupole pole bias as the stopping potential in this experiment was experimentally convenient, but imperfect, since the transmission efficiency of the quadrupole has its own characteristic transfer function as a function of ion energies, typically broadening the resulting stopping potential plot by a two to five eV wide filter. The actual energy distribution of the measured data are actually much narrower than shown here.

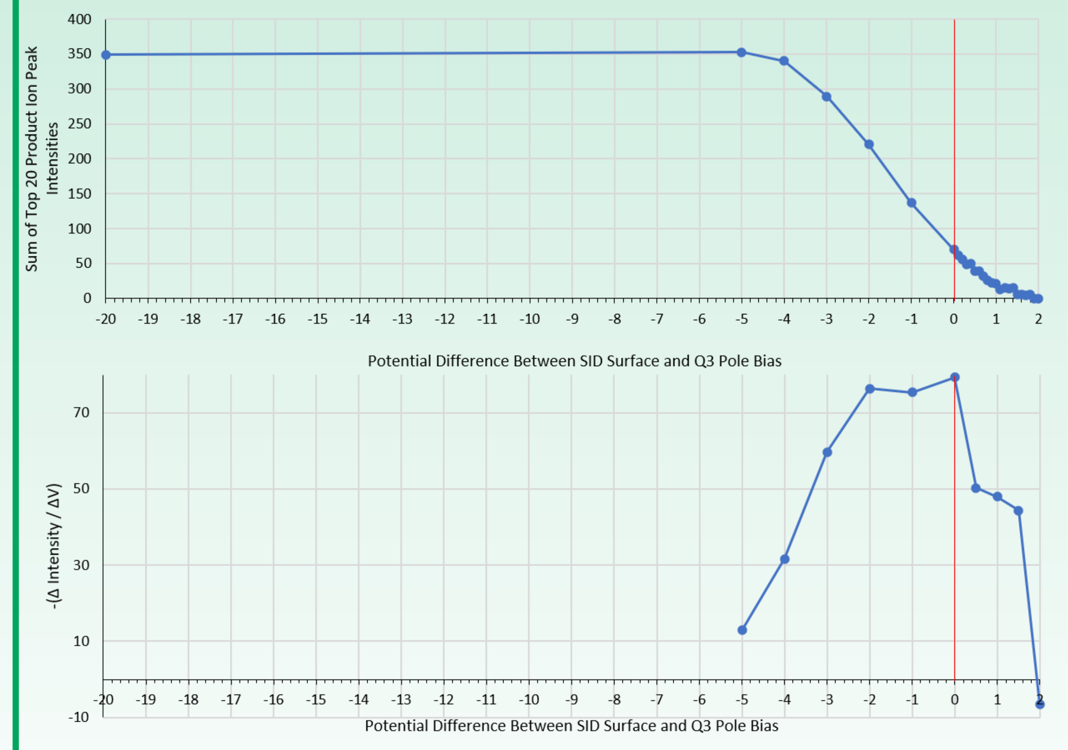


**Figure 11. Stopping potential experiment conducted on the fragment ions produced by SID of [YGGFL+H]$^+$ by varying the pole bias of Q3.**

## Conclusions:

- With Surface Induced Dissociation, the conversion efficiency of parent ions to progeny ions varies from species to species, but was demonstrated to be as high as **~15-20%** for some of the compounds tested in this work. This suggests that SID can be a powerful tool for analytical quantitation.
- The comparison between SID on surfaces of plain stainless steel, versus a self -assembled mononolayer of fluorinated thiol on a copper substrate showed some examples of different fragmentation pathways, which offers additional informing power in a single implementation than using only one of the two substrates, with better overall conversion efficiency seen with the self assembled monolayer surface, as demonstrated previously by other groups.
- The novel use of copper as a substrate for deposition of the self-assembled monolayer surface reduces cost and complexity of SID surface preparation compared with deposition on a gold surface .
- The symmetry of using one surface as a steering lens, and the other as the SID surface offers redundancy in SID operation, effectively doubling the effective surface lifetime between maintenance cycles, while also allowing for system suitability validation of SID performance. By periodically comparing the SID performance of a 'used' surface to the pristine 'gently used' surface, one could validate the viability of the SID surface after extended use.
- The ability to simply and rapidly switch between pass through mode, and SID on either surface offers great potential for comparing the chemistry of SID of differing surfaces, allowing for bracketing experiments to compare the efficacy of different surfaces under identical experimental conditions.
- The stopping potential experiments demonstrate that, for these small molecule parent ions, the progeny ions retain minimal residual ion kinetic energy of the parent, and appear to have the same apparent birth potential across the mass range, which greatly simplifies the need to mass program the pole bias of the second quadrupole, which is often necessary in collision induced dissociation.
- In this experimental configuration, a long (11.850") collision free ion guide was placed between the SID cell and the second quadrupole to help illuminate the timescale of progeny ion 'birth'. If the stopping potential experiment showed a large distribution of ions with an effective birth potential much lower than the surface potential, this would indicate that the ions were 'born' not at the surface potential, rather they would have been born later, somewhere in the ion guide, and the energy distribution would reference the ion guide potential instead of the surface potential. For the small molecules measured in this work, **we conclude that the progeny ions effective birth potential references the surface potential, and therefore that the progeny ions were born quickly after interaction of the parent ion with the surface.**
- This implementation of SID in a tandem mass spectrometer offers a mechanically simple, thin (less than an inch of device thickness), and relatively easy to tune configuration, (only four tuned elements). SID greatly simplifies the overall system design, compared to Collision Induced Dissociation, eliminating the requirement for a bottled collision gas, with its regulators, flow controllers, plumbing and increased gas pumping load, not to mention the RF-only collision cell and its RF power supply, leading to a lighter, more compact system, especially important for portable instruments.
- Using SID for MS/MS using a tandem quadrupole instrument offers the potential for more reproducible, better precision, MS/MS performance than using CID in a traditional ion trap configuration.
- **Serendipity Bonus:** The discovery that split steering lens elements tended to optimize at or near the same potentials allows for the further simplification of the mechanical design, as well as taking away an additional degree of freedom, dramatically simplifying the tuning.

## References:

Bier, M. E.; Amy, J. W.; Cooks, R. G.; Syka, J. E.; Ceja, P.; Stafford, G. A Tandem Quadrupole Mass Spectrometer for the Study of Surface-Induced Dissociation. Int. J. Mass Spectrom. Ion Processes 1987, 77 (1), 31–47.

Wysocki, V. H.; Joyce, K. E.; Jones, C. M.; Beardsley, R. L. Surface-Induced Dissociation of Small Molecules, Peptides, and Non-Covalent Protein Complexes. J. Am. Soc. Mass Spectrom. 2008, 19 (2), 190–208

Fonder, G.; Laffineur, F.; Delhalle, J.; Mekhalif, Z. Alkanethiol-Oxidized Copper Interface: The Critical Influence of Concentration. J. Colloid Interface Sci. 2008, 326 (2), 333–338

COI Disclosure: The authors are employees of Ardara Technologies LP, a manufacturer of mass spectrometers.

Poster reprint requests should be emailed to Info@ArdaraTech.com →